JACS
JOURNAL OF THE AMERICAN CHEMICAL SOCIETY

ARTICLE

pubs.acs.org/JACS

Lyotropic Liquid Crystals Formed from ACHC-Rich β-Peptides

William C. Pomerantz,[†] Virany M. Yuwono,[§] Ryan Drake,[†] Jeffrey D. Hartgerink,[§] Nicholas L. Abbott,[*,‡] and Samuel H. Gellman[*,†]

[†]Department of Chemistry, University of Wisconsin—Madison, 1101 University Avenue, Madison, Wisconsin 53706, United States

[‡]Department of Chemical and Biological Engineering, University of Wisconsin—Madison, 1415 Engineering Drive, Madison, Wisconsin 53706, United States

[§]Department of Chemistry and Bioengineering, Rice University, 6100 Main Street, Houston, Texas 77005, United States

Supporting Information

ABSTRACT: We have examined the effect of β-peptide modifications on the propensity of these helical molecules to form lyotropic liquid crystalline (LC) phases in water. All of the β-peptides we have examined contain 10 residues. In each case, at least three residues are derived from *trans*-2-aminocyclohexanecarboxylic acid (ACHC), which strongly promotes folding to a 14-helical conformation. The structural features varied include the number of ACHC residues, the nature and spatial arrangement of charged side chains (cationic vs anionic), and the identity of groups at the β-peptide termini. We found that relatively small changes (e.g., swapping the positions of a cationic and an anionic side chain) could have large effects, such as abrogation of LC phase formation. The trends revealed by sequence—property studies led to the design of LC-forming β-peptides that bear biomolecular recognition groups (biotin or the tripeptide Arg—Gly—Asp). Structural analysis via circular dichroism and cryo-transmission electron microscopy revealed the existence of two different types of self-associated species, globular aggregates and nanofibers. Nanofibers are the predominant assembly formed at concentrations that lead to LC phase formation, and we conclude that these nanofibers are the functional mesogens. Overall, these studies show how the modularity of β-peptide oligomers enables elucidation of the relationship between molecular structure and large-scale self-assembly behavior.

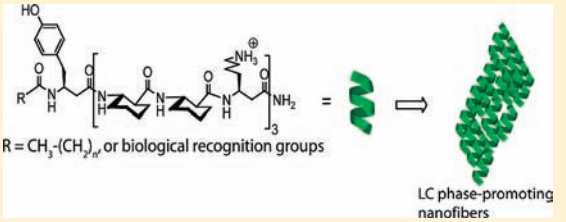

INTRODUCTION

Elucidation of the fundamental rules of molecular self-assembly that lead to formation of well-defined nanostructures enables the rational design of a broad range of new materials.[1−3] A number of recent studies have reported progress toward this goal.[4−8] Of particular relevance to the investigation reported in this Article, Clark et al.[9−11] have recently provided new insights into aromatic interactions that govern the formation of supramolecular nanostructures and organization into liquid crystals (LCs)[12,13] through studies of double-stranded DNA and RNA oligomers that form lyotropic LC phases (solvent-induced LC phases) at high concentrations in water.

Here, we address a second class of bioinspired molecules, short oligomers of β-amino acids (β-peptides), that we and others have recently reported to assemble in aqueous solution into a variety of nanostructures.[14−22] For example, β-peptides synthesized with specific sequences of β-amino acid residues have been reported to form discrete assemblies,[15,17,20,21,23−25] exhibit enzyme-like behavior,[19] form higher-ordered nanostructures,[18,26,27] and participate in sequence-specific interactions at the single molecule level.[28] In addition, a rather diverse set of β-peptide oligomers has been reported to form assemblies that exhibit liquid crystallinity, with LC phase formation depending strongly on the identity and sequence of the β-amino acid residues.[27,29,30] Because oligomers are intrinsically modular, β-peptides constitute a versatile scaffold with which to elucidate sequence—property relationships in LC systems. This class of mesogens may ultimately enable the design of new types of functional LC phases.

Previously, we showed that appropriately designed sequences, with a high proportion of the cyclically constrained residues derived from *trans*-2-aminocyclohexanecarboxylic acid (ACHC; Chart 1), can self-assemble to form LC phases in aqueous solution.[29] Here, we provide a more detailed description of factors governing self-assembly of ACHC-rich β-peptides into nanostructures that form LC phases, and we use this information to design nanostructures that are functionalized with biological recognition groups. Sequence—property studies reveal the importance of the identity and patterning of side-chain functionality in promoting the formation of the LC phases. Structural studies reveal the presence of two distinct nanostructures composed of ACHC-rich β-peptides: at low concentrations, small globular aggregates form, and at high concentrations, high-aspect-ratio nanofibers are generated. These nanofibers appear to be the mesogens that lead to the observed LC phases.

Received: May 26, 2011
Published: August 04, 2011

Chart 1. Globally Amphiphilic β-Peptides 1−4 and Helical Wheel Diagram (View along the Helical Axis) of 1[a]

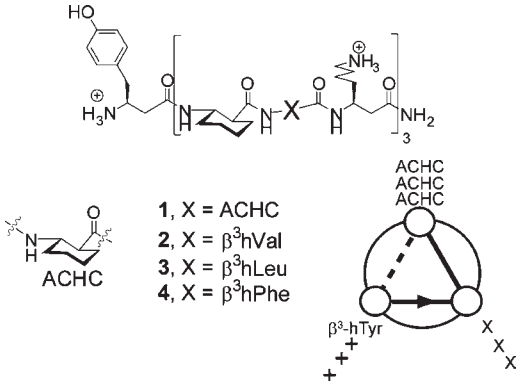

[a]Because the 14-helix has ca. three residues per turn, sequences based on a triad repeat, such as those used here, lead to a helix with three columns of identical side chains running along the sides.

EXPERIMENTAL SECTION

Materials. Fmoc-(*S*,*S*)-*trans*-2-aminocyclohexanecarboxylic acid (Fmoc-*S*,*S*-ACHC) was prepared by the method outlined by Schinnerl et al.[31] Fmoc-(*S*)-β^3-amino acids were prepared from their corresponding α-amino-acids (Novabiochem)[32] or purchased from Peptech. Biotech grade DMF was purchased from Aldrich and stored over 50W-X8 DOWEX ion-exchange resin. Methanol, CH_2Cl_2, tetrahydrofuran, and acetonitrile were purchased from Burdick and Jackson. *O*-Benzotriazol-1-yl-*N*,*N*,*N*′,*N*′-tetramethyluronium hexafluorophosphate and NovaSyn TGR resin (0.25 mmol/g loading) were purchased from Novabiochem. iPr_2EtN was distilled over calcium hydride. All other reagents were purchased from Aldrich and used without purification.

***β*-Peptide Synthesis.** All 14-helical β-peptides were synthesized on solid phase in a CEM MARS microwave reactor. Microwave synthesis was carried out as previously reported.[33] All β-peptides were purified via reverse phase high pressure liquid chromatography (RP-HPLC) on a Vydac C18 semipreparative column using a flow rate of 3 mL/min with a 0.5% B/minute solvent gradient. Solvent A and Solvent B for RP-HPLC were 0.1% trifluoroacetic acid (TFA) in Millipore water and 0.1% TFA in acetonitrile, respectively. Initial purification conditions for the % B solvent gradient (*X*% B to *Y*% B over 20 min) were determined on the basis of the retention time (RT) of the β-peptide in an initial analytical run (flow rate of 1 mL/min from 10% to 60% B over 50 min) using the following equation:

$$X\%\ \text{B to}\ Y\%\ \text{B} = (\text{RT} - 2)\ \text{to}\ (\text{RT} + 8) \quad (1)$$

Final β-peptide purity was assessed using a Vydac C18 analytical column using a flow rate of 1 mL/min from 10% to 60% B over 50 min monitoring at 220 and 273 nm. Purified β-peptides were further characterized by MALDI-TOF-MS (matrix-assisted laser desorption-ionization-time-of-flight mass spectrometry) Further details on synthesis and purification can be found in the Supporting Information.

Polarized Light Optical Microscopy (POM). β-Peptides were weighed into Eppendorf tubes, diluted to the desired concentration with water, and left on an oscillatory shaker overnight to ensure dissolution. β-Peptide solutions were then drawn into a 2 μL microcapillary (0.08 cm o.d., 0.028 cm i.d.; Drummond), and the ends were sealed with a high viscosity vacuum grease (Dow-Corning). Microcapillaries were placed on a glass slide and imaged on an Olympus BX-60 microscope (Tokyo, Japan) in transmission mode between crossed polarizing filters using a digital camera (Olympus C2020 Zoom). To assess if birefringence could be observed at concentrations approaching the solubility limit of each β-peptide, a 1 μL droplet of a concentrated β-peptide solution was allowed to slowly evaporate while being monitored for birefringence.

Variable Temperature ^{2}H NMR. An LC solution of β-peptide **8** was prepared in D_2O (99.9% D, Cambridge Isotope Laboratories, Inc.) and left to agitate overnight. After dissolution, the sample was transferred to a 3 mm NMR tube (Wilmad) and placed in a 500 mHz Varian NMR spectrometer. Spectra of D_2O were recorded as the temperature was varied in 1−5 °C increments, allowing 10 min for equilibration between scans. Spectra were acquired by monitoring deuterium on the lock channel.

Cryo-Transmission Electron Microscopy (Cryo-TEM). A small quantity (typically 3 μL) of the sample solutions (0.2−2.5 wt %) was applied to a TEM copper grid with holey carbon film purchased from Quantifoil (400 mesh Cu grid, 1.2 μM hole diameter) and was blotted with filter paper using a Vitrobot type FP 5350/60 under 100% relative humidity for 2 s to create a thin layer of sample on the surface of the grid. The grid was plunged into liquid ethane and quickly transferred to liquid nitrogen. The sample was analyzed using a JEOL 2010 TEM at an accelerating voltage of 200 kV under low-dose imaging conditions.

Circular Dichroism (CD). Samples were prepared by weighing lyophilized β-peptides into Eppendorf tubes and dissolving in Millipore water to yield 1−2.5 wt % solutions (6−15 mM), which were further diluted to the desired concentrations. The final concentration of each β-peptide solution was determined from the UV absorbance using the extinction coefficient of 1420 cm^{-1} mol^{-1} at 275 nm for α-tyrosine.[34] CD spectra were recorded on an Aviv 202SF spectrometer at room temperature using a 1, a 0.1, or a 0.01 mm path length cell and 3 s averaging times. The CD signal resulting from the water alone was subtracted from the spectrum of each β-peptide solution. Data were converted to mean residue ellipticity (deg cm^2 $dmol^{-1}$) according to the equation:

$$[\Theta] = \Psi/(1000nlc) \quad (2)$$

where Ψ is the CD signal in degrees, n is the number of amides, l is the path length in centimeters, and c is the concentration in decimoles per cm^3.

RESULTS

Role of ACHC in LC Phase Formation. Hydrophobically driven assembly processes are promoted not only by the overall lipophilicity of a molecule but also by specific arrangements of lipophilic elements on the molecular surface and specific associations of lipophilic elements at intermolecular contacts.[2] A specific packing arrangement is seen, for example, in the coiled-coil motif found in proteins. Aliphatic side chains, such as that of leucine, are commonly found to interdigitate in a specific manner at hydrophobic coiled-coil interfaces.[35,36] We attempted to harness a comparable type of packing among 14-helices rich in the cyclic β-amino acid ACHC. The X-ray crystal structure of an ACHC hexamer[37] reveals interdigitation of the cyclohexyl units of neighboring β-peptides, a motif that was termed a "cyclohexyl zipper" (inspired by the use of the term "leucine zipper" to describe coiled-coil dimers). Water-soluble 14-helices displaying an ACHC−ACHC−β^3hLys triad repeat, such as **1** (Chart 1), self-assemble in aqueous solution and form LC phases at high concentration.[29] Because the 14-helix has ca. three residues per turn, this triad repeat generates a helix with a well-defined lipophilic surface and a well-defined hydrophilic surface, as indicated by the helical wheel diagram in Chart 1. We describe this type of helix as being "globally amphiphilic". To determine whether self-assembly to form LC phases is specific for a cyclohexyl zipper motif or generally seen for sequences with different

Chart 2. Acylated β-Peptides Containing Hydrocarbon Acyl Tails, Ac-1 and 5−13, and Biological Recognition Groups, 14 and 15

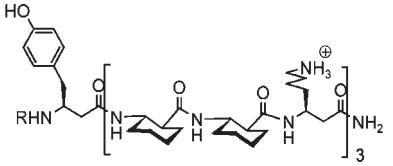

R = CH_3CO-	**Ac-1**	R = C_6H_5CO-	**11**
R = CH_3CH_2CO-	**5**	R = $(CH_3)_3CCO$-	**12**
R = $CH_3(CH_2)_2CO$-	**6**	R = $(CH_3)_2CHCO$-	**13**
R = $CH_3(CH_2)_3CO$-	**7**	R = Biotin-β-hGly	**14**
R = $CH_3(CH_2)_4CO$-	**8**	R = RGD-β-hGly	**15**
R = $CH_3(CH_2)_5CO$-	**9**		
R = $CH_3(CH_2)_6CO$-	**10**		

lipophilic−lipophilic−hydrophilic triad repeats, we examined β-peptides **2** and **3**, in which one set of ACHC residues was replaced with lipophilic β^3-amino acids, either β^3homovaline (β^3hVal) in **2** or β^3homoleucine (β^3hLeu) in **3** (Chart 1). The once-per-triad replacement pattern leads to replacement of a column of ACHC residues with a column of the β^3-residues. In a separate study, we showed that **4**, which has a 14-helical face displaying the aromatic side chains of β^3hPhe, is unable to form an LC phase;[30] however, the aliphatic side chains of β^3hVal and β^3hLeu in **2** and **3** are worthy of evaluation because of their preponderance in many α-peptides that undergo coiled-coil assembly[35] as well as their prominence in recent examples of β-peptide assemblies.[15−17,20,21,25]

Polarized optical microscopy (POM) was used as an initial screen for the formation of LC phases based on the observation of birefringence, an optical property of ordered anisotropic materials. No birefringence was observed for solutions of β-peptide **2** or **3**, indicating that LC phases did not form (Figure S2). The absence of liquid crystallinity among β-peptide analogues of **1** in which an entire column of ACHC residues along one side of the 14-helix is replaced with β^3-amino acid residues supports the hypothesis that LC phase formation results from ACHC-promoted self-assembly. LC behavior is a late-stage read-out for assembly into a particular type of nanostructure; therefore, POM results cannot rule out the possibility that β-peptides **2** and **3** self-assemble into nanostructures that do not result in LC phase formation. Indeed, we previously showed that globally amphiphilic β-peptide **4** self-assembles into small globular aggregates,[30] which do not possess the high aspect ratio necessary for LC phase formation.

Role of Net Charge and Charge Distribution in LC Phase Formation. Prior studies of LC phases composed of ACHC-rich β-peptides revealed that acetylation of the N-terminus, as in **Ac-1** (Chart 2), lowers the concentration range at which the LC phase forms (minimum liquid crystal concentration (MLC) = 2.5 wt % (15 mM) for **Ac-1** vs MLC = 8 wt % (48 mM) for **1**).[29] The significant decrease in the MLC led us to conclude that reduction of the β-peptide net charge (+4 to +3) via N-terminal acetylation of **1** reduced the electrostatic repulsion within the highly aggregated system. To go beyond a simple net charge hypothesis, we have now examined the way in which variations in the spatial patterning of charged groups regulate self-assembly into LC phases. We explored the consequences of replacing β^3hLys at position 10, 7, or 4 of β-peptide **1** with β^3hGlu to generate **K10E-1**, **K7E-1**, or **K4E-1** (Figure 1), each of which is expected to have a net charge of +2 at neutral pH. In addition to a further reduction in net charge relative to **1** (+4) and **Ac-1** (+3), replacement of a positively charged functional group ($-NH_3^+$) with a negatively charged functional group ($-COO^-$) introduces the potential for both inter- and intramolecular attractive interactions (salt bridge formation). In the case of **K10E-1**, with the negatively charged β^3hGlu closest to the C-terminus, the LC phase tolerates the β^3hGlu substitution, but the change in charge state does not improve the propensity for LC phase formation relative to the parent compound (MLC for **K10E-1** = 10 wt % (65 mM) vs MLC for **1** = 8 wt % (48 mM)). Close inspection of the optical texture of the LC phase formed from **K10E-1** showed that the cholesteric phase observed for a solution of **1** is maintained after the β^3hLys10 → β^3hGlu substitution (fingerprint textures, Figure S3). In contrast to **K10E-1**, isomers **K7E-1** and **K4E-1**, which have different placements of the β^3hGlu residue, do not form LC phases at 10 wt % (Figure 1).

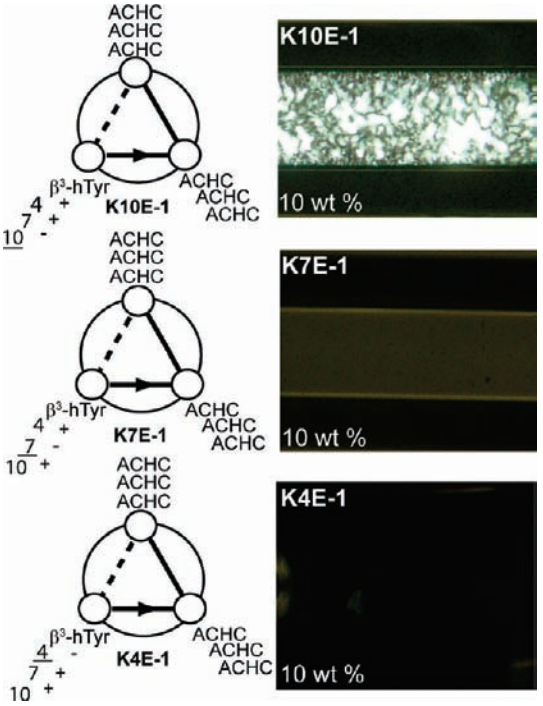

Figure 1. Helical wheel diagrams of the three β^3hLys → β^3hGlu mutants of **1** and corresponding optical micrographs of 10 wt % aqueous solutions between crossed polarizing filters. Dimensions of capillary tubes are 0.08 cm o.d., 0.028 cm i.d.

It is noteworthy that the β^3hLys → β^3hGlu replacements diminish or abolish the propensity for LC formation while N-terminal acetylation enhances LC formation propensity, because the former modifications involve a larger change in net charge than does the latter (+4 to +2 vs +4 to +3), and the larger change should cause a larger decrease in Coulombic repulsion between β-peptide molecules. These observations suggest that it is not net charge but rather the spatial distribution of charged groups on the surface of the helical β-peptide that influences self-assembly behavior. We wondered whether changes at the β-peptide termini have an effect intrinsically different from changes at side chains. To address this question, we prepared β-peptides **1-COOH** and **Ac-1-COOH**, the analogues of **1** and

Figure 2. Optical micrographs of aqueous solutions of acylated β-peptides **7**, **12**, and **13** between crossed polarizing filters. Dimensions of capillary tubes are 0.08 cm o.d., 0.028 cm i.d.

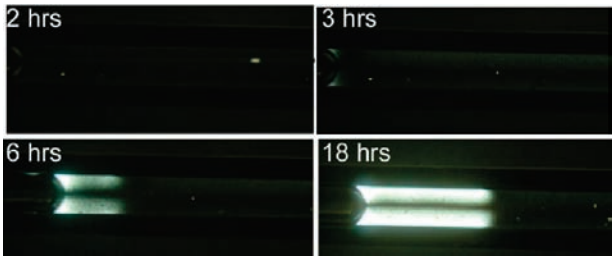

Figure 3. Optical micrographs of a 2.5 wt % aqueous solution of **8** between crossed polarizing filters obtained at various time points. Initial birefringence is observed to occur after 2 h. Dimensions of capillary tubes are 0.08 cm o.d., 0.028 cm i.d.

Ac-1, respectively, that bear an ionizable carboxylic acid (−COOH) at the C-terminus instead of a nonionizable amide group ($CONH_2$). These C-terminal modifications should lead to changes in net charge, from +4 to +3 for **1** → **1-COOH** or +3 to +2 for **Ac-1** → **Ac-1-COOH**. In both cases, changing the C-terminal group led to only small changes in the propensity to form an LC phase: MLC = 9 wt % (54 mM) for **1-COOH** versus 8 wt % (48 mM) for **1**, and MLC = 2 wt % (12 mM) for **Ac-1-COOH** versus 2.5 wt % (15 mM) for **Ac-1**. Thus, these C-terminal changes are comparable to the β^3hLys10 → β^3hGlu change in exerting little discernible impact in terms of the self-assembly that leads to liquid crystallinity. Overall, our observations indicate that net charge reduction at the N-terminus has a significant effect on LC phase formation (**1** vs **Ac-1**), but net charge reduction along the side of the helix can abolish LC phase formation (**1** vs **K4E-1** or **K7E-1**), and net charge reduction at the C-terminus has relatively little effect on LC phase formation (**1** vs **K10E-1** or **1-COOH**; **Ac-1** vs **Ac-1-COOH**).

Role of N-Terminal Acylation in LC Phase Formation. N-Terminal acetylation, as described above, reduces the β-peptide net charge and concomitantly increases net lipophilicity. N-Terminal acylation of conventional peptides with lipophilic groups was previously demonstrated as a strategy for inducing self-assembly of α-helices,[38,39] for collagen-like triple helix assembly,[40−42] and for assembly of extended strands into cylindrical micelles.[43−46] Recently, Müller et al. demonstrated that attaching a seven carbon acyl tail to β-peptide **1** promotes assembly at micromolar concentrations.[19] Therefore, we examined the effects of varying N-terminal acyl groups on LC behavior of β-peptides with the sequence of **1** (Chart 2).

Elongating the acyl tail of **Ac-1** by one methylene (**5**) reduced the concentration necessary to form a LC phase 2.5-fold (MLC for **5** = 1 wt % (5.7 mM) vs MLC for **Ac-1** = 2.5 wt % (15 mM); Figure S1). For both **Ac-1** and **5**, no fingerprint patterns were observed, indicating a loss of the cholesteric phase that is

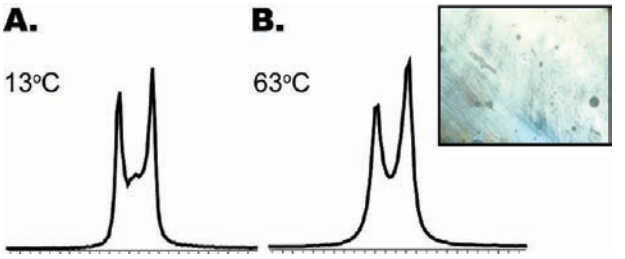

Figure 4. ^{2}H NMR spectra of 2 wt % **8** in D_2O as a function of temperature: (A) 13 °C; (B) 63 °C. Inset: Optical micrograph of 2 wt % **8** in D_2O in a 3 mm NMR tube and obtained at room temperature between crossed polarizing filters.

observed for **1**. Subsequent tail elongation (β-peptides **6**−**9**) did not produce any further lowering of the MLC within the detection limit of this measurement (MLC = 1 wt % in each case; Figures 2 and S1). β-Peptide **10**, possessing the longest acyl tail, had less favorable LC properties (MLC = 2.5 wt % (14 mM), Figure S1). The decrease in MLC, relative to **Ac-1**, for β-peptides with longer, more lipophilic tails (**5**−**9**) may result from a general increased hydrophobic drive for the assembly process. Alternatively, the favorable effect of lipophilic tails on β-peptide assembly may arise from favorable specific types of intermolecular packing arrangements among the tail units.

To begin to address packing effects, we examined the impact of N-terminal lipophilic groups with different shapes by evaluating three β-peptides derived from **1**: **11** (N-terminal benzoyl), **12** (N-terminal pivaloyl), and **13** (N-terminal iso-butanoyl). No birefringence was observed for aqueous solutions of **11** or **12** (Figures 2 and S1), which indicates that the assembly process leading to the LC phase formation is sensitive to the shape of lipophilic groups at the N-terminus. This steric inhibition of LC phase formation could be attenuated by removing one methylene group from the pivaloyl group to generate the iso-butanoyl group (**12** → **13**; Figures 2 and S1).

In addition to affecting the minimum concentration required for LC phase formation, N-terminal acylation can influence the kinetics of LC phase formation. β-Peptide **1** forms the LC phase within minutes after dissolution in water. However, analogous β-peptides possessing lipophilic acyl tails, such as **8** (N-terminal hexanoyl group), can take hours to form a stable LC phase, as monitored by POM (Figure 3). Further changes in the state of the solution cannot be detected after 18 h (no increased birefringence). LC solutions of **8** are stable for months when stored at 4 °C (no precipitation or gelation; birefringence still present).

We investigated the stability of the LC phase formed by **8** as a function of temperature. In a previous study, we examined the temperature-dependent behavior of **1** by ^{2}H NMR. The NMR data indicated that the LC phase of a 10 wt % solution of **1** was fully disrupted at 40 °C (isotropic phase), and that the LC phase reformed within minutes upon cooling. To examine the effects of N-terminal acylation on LC phase thermal stability, we used ^{2}H NMR to examine the LC solution behavior of hexanoylated β-peptide **8**, for comparison with the behavior of **1** (no acyl group).

^{2}H NMR spectra obtained for a 2 wt % solution of **8** (2 × MLC) revealed a doublet resonance characteristic of a nematic phase[47] with a line-shape similar to the doublet from an LC solution of **1** (Figure 4),[29] although a significantly smaller coupling was observed (13 Hz for **8** vs 29 Hz for **1**). Upon heating, there

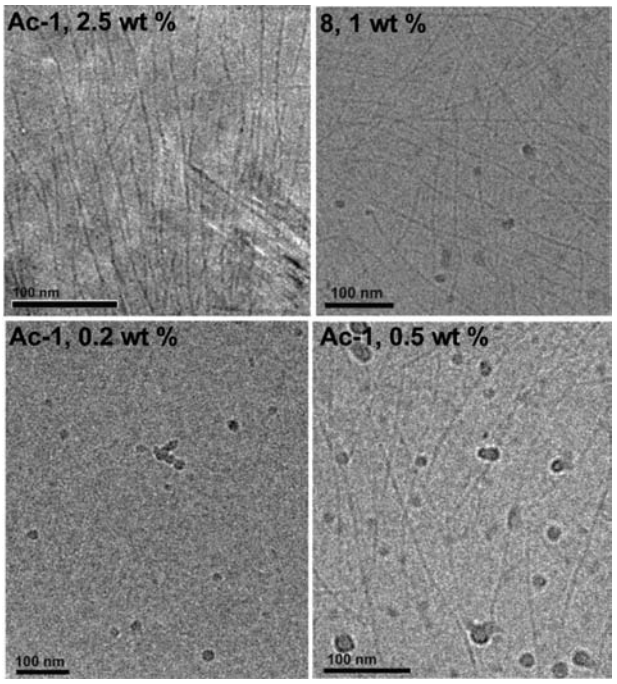

Figure 5. Cryo-TEM electron micrographs of vitrified aqueous solutions of **Ac-1** and **8**.

was little change in the NMR spectrum for **8** over a 50 °C range (Figure 4B). A fully formed LC phase at elevated temperature is suggested by the lack of an isotropic singlet at the maximum temperature; POM data obtained for the NMR sample at room temperature demonstrate the existence of the LC phase under this condition (Figure 4, inset). Below room temperature, a small peak between the peaks of the LC doublet suggests that a small amount of the isotropic phase is present (Figure 4A); however, the intensity of this peak did not increase upon further cooling.

The ^{2}H NMR studies for solutions of **1** and **8** reveal both similarities and differences in mesophase behavior. There is a clear difference in the impact of heating: a LC solution of **8** is relatively unaffected by elevated temperature, while an LC solution of **1** is fully disrupted by heating to 40 °C.[29] However, the similar peak shapes of the D_2O resonance doublets indicate that the mesophases are both nematic: simple nematic in the case of **8** and chiral nematic (i.e., cholesteric) for **1**, at the concentrations used for NMR analysis. A smaller coupling resulting from solutions of **8** relative to couplings observed for solutions of **1** suggests a lower degree of ordering within the LC phase of **8**.

Overall, it appears that N-terminal acylation can affect LC phase formation in several ways including lessening of intermolecular Coulombic repulsion by removal of a positive charge and inhibition of intermolecular association if there is too much steric bulk near the N-terminus. Increasing acyl tail lipophilicity can enhance intermolecular association in water, which may result from a hydrophobic driving force and from favorable packing of the acyl tails in the assembled state. A tightly packed environment for the N-terminus is supported by the observations that bulky lipophilic groups prevent LC phase formation. Finally, the MLC is significantly reduced via removal of the N-terminal positive charge by way of acylation, but not by charge reduction from β^3hLys → β^3hGlu side chain mutations or C-terminal $CONH_2$ → COOH modifications. These observations suggest that the assembly behavior within our family of 14-helical β-peptides is controlled not only by the net charge borne by each molecule, but also by the pattern in which charged groups are displayed on the helical scaffold.

Cryo-TEM Analysis of Solutions of Ac-1 and 8. Onsager theory predicts that particles possessing a high aspect ratio (the mesogens) can spontaneously form an LC phase via excluded volume interactions.[12] Ten-residue 14-helical β-peptides do not possess a sufficiently high aspect ratio (particle length/particle diameter, L/D) to form an LC phase as individual molecules; for these molecules, the helical length is ~1.56 nm and the diameter is ~0.54 nm ($L/D \approx 2.9$),[48] which suggests that self-assembly is required to generate the mesogen. On the basis of Onsager theory, LC formation in a 1 wt % of β-peptide would require that hundreds of β-peptide molecules assemble into a high-aspect-ratio nanostructure.[48]

We used cryogenic transmission electron microscopy (cryo-TEM)[49] to characterize the nanostructures that form in aqueous solutions of **Ac-1** or **8**. Previously, we showed that a nonglobally amphiphilic β-peptide forms high-aspect-ratio nanofibers.[27,30] We therefore wondered whether similar nanostructures could be observed with globally amphiphilic β-peptides such as **Ac-1** or **8**.

Inspection of a vitrified solution of **Ac-1** at the MLC (2.5 wt %) showed a large population of nanofibers (Figure 5, top left). These nanofibers are similar to the nanostructures that we assume to be responsible for LC phase formation by a nonglobally amphiphilic β-peptide.[30] Comparable nanofibers are formed by **8** at the MLC (Figure 5, top right). The nanofibers formed from **Ac-1** and **8** are at least hundreds of nanometers in length. This length appears to be consistent with the mesogen length required by Onsager theory for LC phase formation in the observed concentration range.[48] **Ac-1** and **8** form nanofibers with diamters of ~10 nm (the intrinsically poor contrast of cryo-TEM images limits the resolution). On the basis of the largest dimension of a single β-peptide (~1.6 nm), the fiber thickness indicates that at least five or six β-peptides are necessary to span the diameter of the fiber. The similarity in fiber diameters observed for **Ac-1** and **8** suggests that variation in the β-peptide acyl tail (acetyl in **Ac-1** vs hexanoyl in **8**) does not exert an observable effect on fiber thickness, and therefore from the data available, analysis of the nanofiber aspect ratios cannot be used to explain the differences in MLC.

We examined the impact of changing concentration on the nanostructures formed in solutions of **Ac-1** or **8**. Only globular aggregates are observed at 0.2 wt % **Ac-1**, which is below the MLC (Figure 5, bottom left). Increasing the concentration of **Ac-1** to 0.5 wt % leads to solutions of **Ac-1** containing both nanofibers and globular aggregates (Figure 5, bottom right). Only nanofibers are observed when the concentration of **Ac-1** reaches the MLC (2.5 wt %; Figure 5, top left). Cryo-TEM images of solutions of **8** indicate nanofiber formation at concentrations as low as 0.2 wt % (Figure S6). Globular aggregates are also present, but at much lower levels than is observed for solutions of **Ac-1** (Figure 5, top right and Figure S6).

The cryo-TEM data suggest that there is a concentration-dependent equilibrium between two different types of nanostructures, globular aggregates and nanofibers. At low β-peptide concentrations, the equilibrium favors formation of globular aggregates; however, increasing concentration leads to coexistence of globular aggregates and nanofibers. At sufficiently high concentrations, beyond the MLC, nanofibers are the dominant aggregate form, and a dense, ordered nanofiber network is

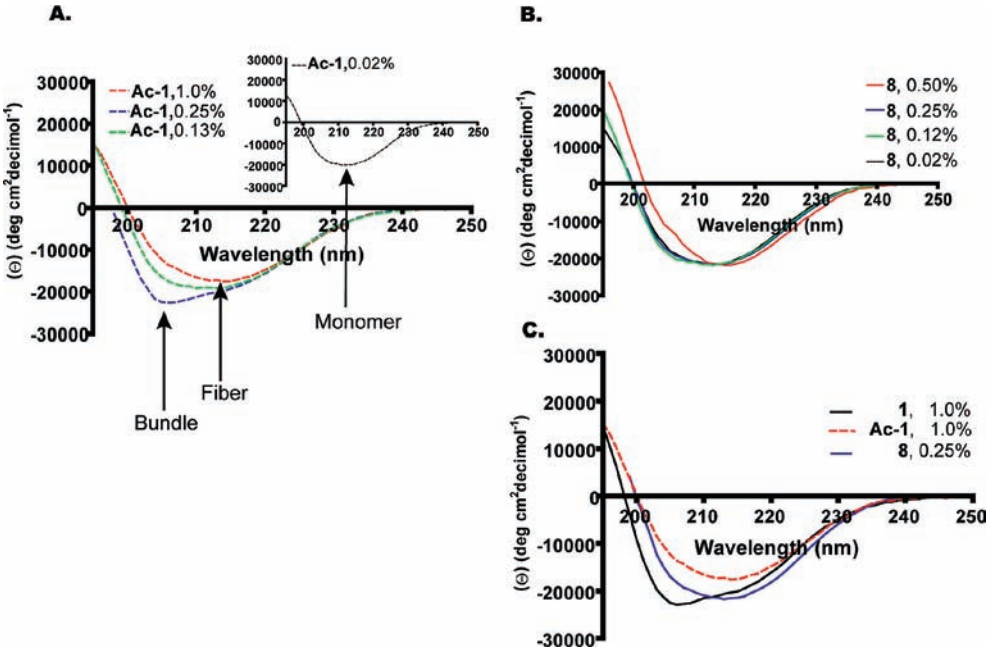

Figure 6. CD spectra of β-peptides as a function of concentration in aqueous solution. (A) **Ac-1**, 0.02−1.0 wt %, increased molar ellipticity at 205 nm correlates with helical bundle formation; (B) **8**, 0.02−0.50 wt %; and (C) **1**, 1 wt %, **Ac-1**, 1 wt %; and **8**, 0.25 wt %. Only **1** shows evidence of significant bundle formation at 1 wt %.

observed. Given the similarities in nanofiber dimensions for **Ac-1** and **8**, we conclude that **8** forms LC phases at lower concentrations than does **Ac-1** because nanofibers of **8** are more stable than (and hence form at lower concentrations than) nanofibers of **Ac-1**.

CD Analysis of β-Peptides 1, Ac-1, and 8. Our initial design hypotheses were based on the premise that the β-peptides we used adopt 14-helical conformations. However, highly α-helical proteins have been shown to form β-sheet aggregates under denaturing conditions,[50] and sheet secondary structure has been shown to promote fiber formation and LC phases among α-peptides.[4,51−53] We therefore wondered whether our β-peptides might be nonhelical in the assembled state. β-Peptides with a high content of ACHC residues retain the 14-helical conformation under a variety of conditions (e.g., aqueous solution, high temperature, high salt concentration, high urea concentration),[54,55] and we sought to determine whether these molecules adopt 14-helical conformations at concentrations necessary to form nanofibers and produce LC phases. We used circular dichroism (CD) to address this question. CD has been used extensively to characterize β-peptide secondary[56,57] tertiary,[58] and quaternary structure.[59] Therefore, CD can provide information regarding the assembly behavior of β-peptides observed via cryo-TEM and POM.

Helix-bundle-self-assembly of β-peptides has recently been correlated with a pronounced CD minimum near 205 nm, while monomeric 14-helices are characterized by a minimum near 214 nm.[59] The ratio of the signal intensities at 205 nm ($[\theta]_{205}$) and 214 nm ($[\theta]_{214}$) can thus be used to characterize self-assembly into bundles, which appears to be indicated by $[\theta]_{205}/[\theta]_{214} > 0.7$.[59] Nanofiber assemblies have been reported to display CD spectra similar to those of monomeric 14-helices, with $[\theta]_{205}/[\theta]_{214} \leq 0.7$.[30,59] Recently, a 14-helix bundle was reported to display a minimum at 214 nm,[24] which contrasts with previous β-peptide helix bundle results.[11−15] Therefore, CD data alone allow only tentative conclusions regarding β-peptide self-assembly. However, CD can provide a useful complement to other measurements, such as cryo-TEM and POM.

Table 1. CD Molar Ellipticity Ratios of β-Peptides 1, Ac-1, and 8 as a Function of Concentration

β-peptide	concentration (wt %)	$[\theta]_{205}/[\theta]_{214}$	MLC (wt %)
1	1.0	1.1	8
Ac-1	1.0	0.70	2.5
Ac-1	0.25	1.1	2.5
Ac-1	0.13	0.86	2.5
Ac-1	0.02	0.81	2.5
8	0.50	0.50	1
8	0.25	0.79	1
8	0.13	0.83	1
8	0.02	0.74	1

We analyzed β-peptides **1**, **Ac-1**, and **8** via CD over a range of concentrations for comparison with cryo-TEM and POM data. CD spectra of **Ac-1** and **8** at concentrations well below the onset of liquid crystallinity (0.02 wt %) show the characteristic minimum of the 14-helix at 214 nm and lack a second minimum at 205 nm (Figure 6, Table 1). However at a slightly higher concentration of **Ac-1**, 0.13 wt % (0.7 mM), still below the MLC, a new signature is observed with a minimum emerging at 205 nm ($[\theta]_{205}/[\theta]_{214}$ = 0.86; Figure 6A, Table 1). This minimum becomes more pronounced with a further concentration increase to 0.25 wt % (1.4 mM; $[\theta]_{205}/[\theta]_{214}$ = 1.1; Figure 6A, Table 1). The minimum at 205 nm, indicative of helical bundles,[59] correlates with the presence of globular aggregates observed via cryo-TEM. However, at 1 wt % **Ac-1**, a more canonical 14-helical signature is observed ($[\theta]_{205}/[\theta]_{214}$ = 0.70; Figure 6A, Table 1). We interpret this second change in the CD spectrum (reversion to a 14-helical signature) to reflect the formation of nanofibers, as observed by cryo-TEM. This assignment is

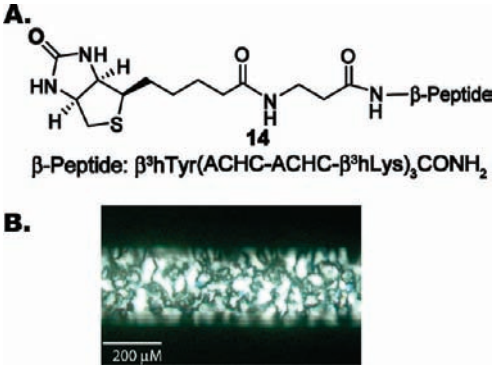

Figure 7. (A) Structure of biotin-functionalized β-peptide **14**. (B) Optical micrograph of a 6 wt % aqueous solution of **14** between crossed polarizing filters revealing nematic schlieren textures. Dimensions of capillary tubes are 0.08 cm o.d., 0.028 cm i.d.

consistent with past observations of β-peptides that form nanofibers.[30]

In contrast to **Ac-1**, **8** does not show a significant deviation from the 14-helical CD signature at any of several concentrations between 0.02 and 0.50 wt % (Figure 6B, Table 1). Cryo-TEM data (Figure 5) indicate that even at 0.2 wt % (well below the MLC, which is 1 wt % for **8**), nanofibers are the dominant aggregate form. It is possible that globular aggregates are never a dominant aggregation state for **8**, or that we did not happen to obtain CD or cryo-TEM data in the narrow concentration range in which globular aggregates are dominant.

CD spectra of unacylated β-peptide **1** show $[\theta]_{205}/[\theta]_{214}$ = 1.1 at concentrations as high as 1 wt % (Figure 6C, Table 1), which suggests the existence of globular aggregates at this concentration. In comparison, $[\theta]_{205}/[\theta]_{214}$ = 0.7 for a 1 wt % solution of **Ac-1**, which is consistent with a predominantly nanofiber state. Because globular aggregates are incompatible with LC phase formation, a higher $[\theta]_{205}/[\theta]_{214}$ for 1 wt % **1** relative to 1 wt % **Ac-1** is consistent with the trend in MLC (8 wt % for **1** vs 2.5 wt % for **Ac-1**). Overall, the CD data are consistent with cryo-TEM data in showing that β-peptide **Ac-1** can form two different types of assembly, depending on concentration: globular assemblies or nanofibers. The latter are favored at higher concentrations. CD data also support the formation of globular aggregates for solutions of **1**. It is not clear from our data whether globular aggregates of **8** are the favored assembly form at any concentration.

Incorporation of Biological Epitopes into β-Peptide LC Phases. The modular nature of β-peptides affords an opportunity to engineer functional components into β-peptide LC phases. The studies described above reveal that a variety of lipophilic acyl tails can be incorporated at the N-terminus of **1** without preventing LC phase formation. As a first step toward engineering functional LC mesogens, we prepared β-peptides bearing either of two recognition groups commonly used in biotechnology: biotin, which binds strongly to streptavidin, or the tripeptide Arg–Gly–Asp, which is specific for integrin receptors on cell surfaces.[60] The resulting β-peptides, **14** and **15** (Chart 2), contain a β-hGly spacer adjacent to the terminal recognition group, based on our observation reported above that steric bulk is not tolerated at the N-terminus. LC phases could be formed from both **14** and **15**, albeit at higher concentrations than are required for β-peptide analogues bearing simple aliphatic acyl groups at the N-terminus (Figures 7 and S5). The higher MLCs of **14** and **15** (6 and 13 wt %, respectively) relative to **5**–**10** may reflect differences between the linear hydrocarbon tails of the latter and the more complex tails of the former (e.g., larger size and more polarity in the tails of **14** and **15**). These two examples establish the feasibility of incorporating biological epitopes into LC phases formed from non-natural components in water and to our knowledge are one of the first reported examples of synthetic lyotropic LC mesogens functionalized with biological epitopes. In the future, lyotropic LCs functionalized with biological epitopes may facilitate the design of biologically responsive materials.[61−64] We envision functionalized nanostructures to have even broader utility in the context of tissue engineering,[46] membranes,[65] and catalysis.[65]

DISCUSSION

ACHC-rich β-peptides are able to form LC phases at low to moderate concentrations in aqueous solution. Through sequence–property studies, we investigated how subtle changes of side-chain functionality and terminal modification affect the ability of β-peptides to self-assemble into higher-ordered structures and produce LC phases. In some cases, we have observed LC phases at concentrations as low as 1 wt % (6 mM) in water. The MLC values for our β-peptides compare favorably to MLC values reported for other agents that form aqueous lyotropic liquid crystals, such as chromonic mesogens (e.g., DSCG, for which the MLC is 10 wt % at room temperature).[66] An MLC of 1 wt % is superior to MLC values observed for ionic surfactants, which range from 10 to >90 wt %[67] (typically ~50 wt %).[68] Small DNA oligomers and water-soluble α-helical α-peptides form LC phases, but only at high concentrations (DNA, 6–20 mers ~90–20 wt %;[10] α-helical α-peptides, M_w = 62–120 kDa, 48–19 wt %[69]). Aggeli et al. have designed a series of self-assembling β-sheet forming peptides that form LC phases at lower concentrations but over a narrow concentration range (1–4 mM before gelation).[4] LC phases generated from peptides at higher concentration took several weeks to form. Zhang et al. reported self-assembly of peptide-amphiphiles leading to lyotropic LC phases at low concentrations when aligned, although these samples form gels.[8]

The sequence–property studies described here elucidate several important design guidelines for generating 14-helical β-peptides that self-assemble into high-aspect-ratio nanofibers that can form LC phases. First, for the class of β-peptides discussed here, it is important to place ACHC at approximately two-thirds of the positions, and these residues must be arranged so that they form a unified surface on the 14-helix (triad sequence repeat). On the basis of X-ray crystallographic data, we propose that a hydrophobic interface between ACHC residues on different β-peptide molecules can facilitate a cyclohexyl-zipper-like motif.[37] Previous studies revealed that globally amphiphilic 14-helical β-peptides containing alternative hydrophobic side chains did not self-assemble into nanostructures leading to LC phases.[30] Second, Coulombic interactions among β-peptide molecule influence their self-assembly, but there is not a simple correlation between net charge and propensity to form an LC phase. The location of charged groups on the β-peptide surface seems to be an important factor, but further work will be required to elucidate in detail how three-dimensional patterning of charged groups influences self-assembly. Third, placing medium-length straight-chain acyl tails at the β-peptide N-terminus enhances

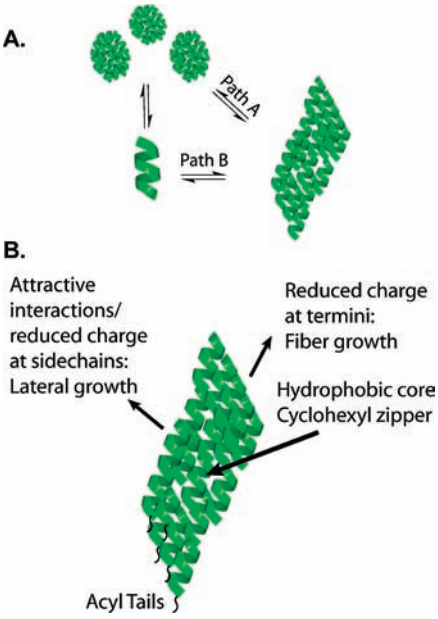

Figure 8. (A) Model for the multistate assembly of globally amphiphilic β-peptides, progressing from monomer to globular aggregate to nanofiber, path A, or through formation of nanofibers directly from monomeric β-peptides, path B. (B) Rationale for β-peptide arrangement within nanofibers, based on sequence−property data reported in this Article.

the propensity for LC phase formation. However, sterically bulky acyl tails (e.g., pivaloyl or benzoyl groups) can prevent LC phase formation. These guidelines enabled us to design β-peptides that can form an LC phase while displaying a biological epitope.

Our observations suggest the outlines of a model for the β-peptide assembly that underlies LC phase formation (Figure 8). Our model is consistent with our POM, cryo-TEM, CD, and previous X-ray crystallography data.[37] Cryo-TEM and CD raise the possibility of a concentration-dependent multistate assembly process that involves globular aggregates at intermediate concentrations and high-aspect-ratio nanofibers at higher concentrations. Small bundles of β-peptides are hypothesized to stack end-to-end forming micrometer-long nanofibers. However, we acknowledge that at present we do not have any data that would allow us to distinguish between the hypothesis in Figure 8, in which the globular aggregates form at intermediate concentrations along an equilibrium pathway that leads to nanofibers at high concentration (path A), and an alternative hypothesis in which both globular aggregates and nanofibers are formed directly from monomeric β-peptides (i.e., a hypothesis in which globular aggregates are not an intermediate on the equilibrium pathway to nanofibers but rather an alternative mode of monomer assembly relative to nanofibers, path B).

We propose that elimination of charge at the N-terminus (N-terminal acylation of **1**) facilitates growth along the fiber axis through reduction of electrostatic repulsion. Alternatively, incorporating side chains that can be negatively charged (as in the β^3hGlu-containing derivatives of **1**) introduces the potential for attractive side-to-side interactions between 14-helical β-peptides. In our proposed model for assembly, such an attractive interaction would promote lateral growth of the nanofibers. This lateral growth would reduce the aspect ratio of the assembly, which is unfavorable for LC phase formation. This structural hypothesis is consistent with a recent study from Dong et al.[70] that showed that reducing charge along the sides of self-assembling coiled-coils significantly affects fiber thickness.

The β-peptides in our study were designed to undergo a hydrophobically driven assembly process with interdigitating ACHC residues at the interface between neighboring β-peptides. Offsetting the registry of interdigitating residues at the hydrophobic interface provides unpaired ACHC residues for subsequent elongation into nanofibers. This assembly hypothesis predicts that globally amphiphilic β-peptides such as **1**, in which the ACHC residues are segregated on one side of the helical conformation and hydrophilic residues are segregated on the other side, will be prone to self-assemble in a manner that leads to LC phase formation. This assembly hypothesis further predicts that sequence-isomeric β-peptides that do not achieve well-defined segregation of ACHC residues and hydrophilic residues in the helical conformation should be less prone to self-assembly in aqueous solution and should not form LC phases. We have previously documented the expected behavior for a nonglobally amphiphilic sequence isomer of **1**.[22,29]

Our β-peptide assembly model is consistent with crystal packing behavior observed for both α- and β-peptides, where helices associate end-to-end to satisfy hydrogen-bonding groups at their termini.[37,71] These head-to-tail arrangements are favored by interactions between the net dipoles of neighboring helices.[72] Our model is similar in several aspects to the self-assembly of DNA oligomers, which form LC phase necessitating both end-to-end stacking as well as interdigitation of aromatic bases for elongation into extended fibers.[9,10]

CONCLUSIONS

By analyzing the ways in which changes in the covalent structure of ACHC-rich β-peptides influence higher order assembly behaviors in solution, we have uncovered several design rules for creating lyotropic LC phases with these molecules. Self-assembly of ACHC-rich β-peptides leads to nanofibers that serve as the LC mesogens. Nanofiber formation may be a multistep process involving multiple modes of β-peptide association. Ultimately, we hope to take advantage of the control over side chain display and aggregate morphology that can be achieved with β-peptides to design LC phases with useful properties. As a first step toward this goal, we have designed β-peptides containing biological recognition groups that can form LC phases.

We recently demonstrated that lyotropic LC solutions of **9** are useful NMR alignment media for small organic molecules in aqueous solution and provided initial evidence for enantiodiscrimination.[73] Additional examples in the literature have shown nanofibers and lyotropic LCs to be useful for nanocrystal templation,[74] biological sensing,[61−64] and NMR RDC analysis.[75−77] Future research based on the LC systems discussed here will explore such applications.

ASSOCIATED CONTENT

Supporting Information. Supplemental figures and experimental details regarding β-peptide synthesis, polarizing optical microscopy, circular dichroism, cryo-TEM, and nanostructure analysis. This material is available free of charge via the Internet at http://pubs.acs.org.

AUTHOR INFORMATION

Corresponding Author
gellman@chem.wisc.edu; abbott@.engr.wisc.edu

ACKNOWLEDGMENT

This research was supported by the UW−Madison Nanoscale Science and Engineering Center (NSF grant DMR-0832760). We thank PepTech for providing several β-amino acids at a discounted price.

REFERENCES

(1) Kato, T. *Science* **2002**, *295*, 2414–8.
(2) Whitesides, G. M.; Mathias, J. P.; Seto, C. T. *Science* **1991**, *254*, 1312–9.
(3) Israelachvili, J. N.; Mitchell, D. J.; Ninham, B. W. *Biochim. Biophys. Acta* **1977**, *470*, 185–201.
(4) Aggeli, A.; Nyrkova, I. A.; Bell, M.; Harding, R.; Carrick, L.; Mcleish, T. C. B.; Semenov, A. N.; Boden, N. *Proc. Natl. Acad. Sci. U.S.A.* **2001**, *98*, 11857–62.
(5) Kokkoli, E.; Mardilovich, A.; Wedekind, A.; Rexeisen, E. L.; Garg, A.; Craig, J. A. *Soft Matter* **2006**, *2*, 1015–24.
(6) Nagarkar, R. P.; Hule, R. A.; Pochan, D. J.; Schneider, J. P. *Biopolymers* **2010**, *94*, 141–55.
(7) Sarikaya, M.; Tamerler, C.; Jen, A. K.-Y.; Schulten, K.; Baneyx, F. *Nat. Mater.* **2003**, *2*, 577–85.
(8) Zhang, S. M.; Greenfield, M. A.; Mata, A.; Palmer, L. C.; Bitton, R.; Mantei, J. R.; Aparicio, C.; de la Cruz, M. O.; Stupp, S. I. *Nat. Mater.* **2010**, *9*, 594–601.
(9) Zanchetta, G.; Giavazzi, F.; Nakata, M.; Buscaglia, M.; Cerbino, R.; Clark, N. A.; Bellini, T. *Proc. Natl. Acad. Sci. U.S.A.* **2010**, *107*, 17497–502.
(10) Nakata, M.; Zanchetta, G.; Chapman, B. D.; Jones, C. D.; Cross, J. O.; Pindak, R.; Bellini, T.; Clark, N. A. *Science* **2007**, *318*, 1276–9.
(11) Zanchetta, G.; Bellini, T.; Nakata, M.; Clark, N. A. *J. Am. Chem. Soc.* **2008**, *130*, 12864–+.
(12) Onsager, L. *Ann. N. Y. Acad. Sci.* **1949**, *51*, 627–59.
(13) Flory, P. J. *Proc. R. Soc. London, Ser. A* **1956**, *234*, 73–89.
(14) Huc, I.; Guichard, G. *Chem. Commun.* **2011**, *47*, 5933–41.
(15) Daniels, D. S.; Petersson, E. J.; Qiu, J. X. *J. Am. Chem. Soc.* **2007**, *129*, 1532–3.
(16) Goodman, C. M.; Choi, S.; Shandler, S.; Degrado, W. F. *Nat. Chem. Biol.* **2007**, *3*, 252–62.
(17) Goodman, J. L.; Molski, M. A.; Qiu, J.; Schepartz, A. *ChemBioChem* **2008**, *9*, 1576–8.
(18) Martinek, T. A.; Hetenyi, A.; Fulop, L.; Mandity, I. M.; Toth, G. K.; Dekany, I.; Fulop, F. *Angew. Chem., Int. Ed.* **2006**, *45*, 2396–400.
(19) Muller, M. M.; Windsor, M. A.; Pomerantz, W. C.; Gellman, S. H.; Hilvert, D. *Angew. Chem., Int. Ed.* **2009**, *48*, 922–5.
(20) Petersson, E. J.; Craig, C. J.; Daniels, D. S.; Qiu, J. X.; Schepartz, A. *J. Am. Chem. Soc.* **2007**, *129*, 5344–45.
(21) Petersson, E. J.; Schepartz, A. *J. Am. Chem. Soc.* **2008**, *130*, 821–3.
(22) Raguse, T. L.; Lai, J. R.; LePlae, P. R.; Gellman, S. H. *Org. Lett.* **2001**, *3*, 3963–6.
(23) Goodman, J. L.; Petersson, E. J.; Daniels, D. S.; Qiu, J. X.; Schepartz, A. *J. Am. Chem. Soc.* **2007**, *129*, 14746–51.
(24) Molski, M. A.; Goodman, J. L.; Craig, C. J.; Meng, H.; Kumar, K.; Schepartz, A. *J. Am. Chem. Soc.* **2010**, *132*, 3658–9.
(25) Korendovych, I. V.; Kim, Y. H.; Ryan, A. H.; Lear, J. D.; DeGrado, W. F.; Shandler, S. J. *Org. Lett.* **2010**, *12*, 5142–5.
(26) Kwon, S.; Jeon, A.; Yoo, S. H.; Chung, I. S.; Lee, H. S. *Angew. Chem., Int. Ed.* **2010**, *49*, 8232–6.
(27) Pizzey, C. L.; Pomerantz, W. C.; Sung, B.-J.; Yuwono, V. M.; Hartgerink, J. D.; Gellman, S. H.; Abbott, N. L. *J. Chem. Phys.* **2008**, *129*, 095103-1–8.
(28) Acevedo-Velez, C.; Andre, G.; Dufrene, Y. F.; Gellman, S. H.; Abbott, N. L. *J. Am. Chem. Soc.* **2011**, *133*, 3981–8.
(29) Pomerantz, W. C.; Gellman, S., H.; Abbott, N. L. *J. Am. Chem. Soc.* **2006**, *128*, 8730–1.
(30) Pomerantz, W. C.; Yuwono, V. M.; Pizzey, C. L.; Hartgerink, J. D.; Abbott, N. L.; Gellman, S. H. *Angew. Chem., Int. Ed.* **2008**, *47*, 1241–4.
(31) Schinnerl, M.; Murray, J. K.; Langehan, J. M.; Gellman, S. H. *Eur. J. Org. Chem.* **2003**, 721–6.
(32) Seebach, D.; Overhand, M.; Kuhnle, F. M. N.; Martinoni, B.; Oberer, L.; Hommel, U.; Widmer, H. *Helv. Chim. Acta* **1996**, *79*, 913.
(33) Murray, J. K.; Gellman, S. H. *Org. Lett.* **2005**, *7*, 1517–20.
(34) Creighton, T. E. *Proteins: Structures and Molecular Principles*, 2nd ed.; W.H. Freeman and Co.: New York, 1993.
(35) Mason, J. M.; Arndt, K. M. *ChemBioChem* **2004**, *5*, 170–6.
(36) Oshea, E. K.; Klemm, J. D.; Kim, P. S.; Alber, T. *Science* **1991**, *254*, 539–44.
(37) Appella, D. H.; Christianson, L. A.; Karle, I.; Powell, D. R.; Gellman, S. H. *J. Am. Chem. Soc.* **1996**, *118*, 13071–2.
(38) Forns, P.; Lauer-Fields, J. L.; Gao, S.; Fields, G. B. *Biopolymers* **2000**, *54*, 531–46.
(39) Malkar, N. B.; Lauer-Fields, J. L.; Juska, D.; Fields, G. B. *Biomacromolecules* **2003**, *4*, 518–28.
(40) Berndt, P.; Fields, G. B.; Tirrell, M. *J. Am. Chem. Soc.* **1995**, *117*, 9515–22.
(41) Yu, Y.-C.; Tirrell, M.; Fields, G. B. *J. Am. Chem. Soc.* **1998**, *120*, 9979–82.
(42) Yu, Y.-C.; Berndt, P.; Tirrell, M.; Fields, G. B. *J. Am. Chem. Soc.* **1996**, *118*, 12515–20.
(43) Silva, G. A.; ZCzeisler, C.; Niece, K. L.; Beniash, E.; Harrington, D. A.; Kessler, J. A.; Stupp, S. I. *Science* **2004**, *303*, 1352–5.
(44) Hartgerink, J. D.; Beniash, E.; Stupp, S. I. *Proc. Natl. Acad. Sci. U.S.A.* **2002**, *99*, 5133–8.
(45) Hartgerink, J. D.; Beniash, E.; Stupp, S. I. *Science* **2001**, *294*, 1684–8.
(46) Jun, H.-W.; Paramonov, S. E.; Hartgerink, J. D. *Soft Matter* **2006**, *2*, 177–81.
(47) Blackburn, J. C.; Kilpatrick, P. K. *Langmuir* **1992**, *8*, 1679–87.
(48) Please see the Supporting Information.
(49) Cui, H.; Hodgdon, T. K.; Kaler, E. W.; Abezgauz, L.; Danino, D.; Lubovsky, M.; Talmon, Y.; Pochan, D. J. *Soft Matter* **2007**, *3*, 945–55.
(50) Dobson, C. M. *Nature* **2003**, *426*, 884–90.
(51) Aggeli, A.; Bell, M.; Boden, N.; Carrick, L.; Strong, A. E. *Angew. Chem., Int. Ed.* **2003**, *42*, 5603–6.
(52) Aggeli, A.; Bell, M.; Carrick, L. M.; Fishwick, C. W. G.; Harding, R.; Mawer, P. J.; Radford, S. E.; Strong, A. E. *J. Am. Chem. Soc.* **2003**, *125*, 9619–28.
(53) Aggeli, A.; Nyrkova, I. A.; Bell, M.; Carrick, L.; Mcleish, T. C. B.; Semenov, A. N.; Boden, N. Exploiting Peptide Self-Assembly to Enginneer Novel Bio-Polymers: Tapes, Ribbons, Fibrils, and Fibers. In *Self-Assembling Peptide Systems in Biology, Medicine and Engineering*; Aggeli, A., Boden, N., Zhang, S., Eds.; Kluwer Academics: Norwell, MA, 2001.
(54) Lee, M. R.; Raguse, T. L.; Schinnerl, M.; Pomerantz, W. C.; Wang, X. D.; Wipf, P.; Gellman, S. H. *Org. Lett.* **2007**, *9*, 1801–4.
(55) Appella, D. H.; Barchi, J. J.; Durell, S. R.; Gellman, S. H. *J. Am. Chem. Soc.* **1999**, *121*, 2309–10.
(56) Cheng, R. P.; Gellman, S. H.; DeGrado, W. F. *Chem. Rev.* **2001**, *101*, 3219–32.
(57) Kritzer, J. A.; Tirado-Rives, J.; Hart, S. A.; Lear, J. D.; Jorgensen, W. L.; Schepartz, A. *J. Am. Chem. Soc.* **2005**, *127*, 167–78.
(58) Cheng, R. P.; DeGrado, W. F. *J. Am. Chem. Soc.* **2002**, *124*, 11564–5.
(59) Pomerantz, W. C.; Grygiel, T. L. R.; Lai, J. R.; Gellman, S. H. *Org. Lett.* **2008**, *10*, 1799–802.

(60) Pierschbacher, M. D.; Ruoslahti, E. *Nature* **1984**, *309*, 30–3.
(61) Van Nelson, J. A.; Seung-Ryeol, K.; Abbott, N. L. *Langmuir* **2002**, *18*, 5031–5.
(62) Shiyanovskii, S. V.; Schneider, T.; Smalyukh, I. I.; Ishikawa, T.; Niehause, G. D.; Doane, K. J.; Woolverton, C. J.; Lavrentovitch, O. D. *Phys. Rev. E* **2005**, *71*, 020702−1–5−5.
(63) Luk, Y.-Y.; Jang, C.-H.; Cheng, L.-L.; Israel, B. A.; Abbott, N. L. *Chem. Mater.* **2005**, *17*, 4774–82.
(64) Cheng, L. L.; Luk, Y. Y.; Murphy, C. J.; Israel, B. A.; Abbott, N. L. *Biomaterials* **2005**, *26*, 7173–82.
(65) Gin, D. L.; Gu, W.; Pindola, B. A.; Zhou, W.-J. *Acc. Chem. Res.* **2001**, *34*, 973–80.
(66) Lydon, J. *Curr. Opin. Colloid Interface Sci.* **2004**, *3*, 480–90.
(67) Kelker, H.; Hatz, R. *Handbook of Liquid Crystals*; Verlag Chemie: Weinheim, 1980.
(68) Collings, P. J. *Liquid Crystals: Nature's Delicate Phase of Matter*, 2nd ed.; Princeton University Press: Princeton, 2002.
(69) Bellomo, E. G.; Davidson, P.; Imperor-Clerc, M.; Deming, T. J. *J. Am. Chem. Soc.* **2004**, *126*, 9101–5.
(70) Dong, H.; Paramonov, S. E.; Hartgerink, J. D. *J. Am. Chem. Soc.* **2008**, *130*, 13691–5.
(71) Karle, I. *Acta Crystallogr.* **1992**, *B48*, 341–56.
(72) Miller, C. A.; Hernandez-Ortiz, J. P.; Abbott, N. L.; Gellman, S. H.; de Pablo, J. J. *J. Chem. Phys.* **2008**, *129*, 05102−1–10.
(73) Thiele, C. M.; Pomerantz, W. C.; Abbott, N. L.; Gellman, S. H. *Chem. Commun.* **2011**, *47*, 502–4.
(74) Lee, S. W.; Mao, C. B.; Flynn, C. E.; Belcher, A. M. *Science* **2002**, *296*, 892–5.
(75) Bax, A.; Kontaxis, G.; Tjandra, N. *Methods Enzymol.* **2001**, *339*, 127–74.
(76) Merlet, D.; Ancian, B.; Courtieu, J.; Lesot, P. *J. Am. Chem. Soc.* **1999**, *121*, 5249–58.
(77) Thiele, C. M. *Concepts Magn. Reson., Part A* **2007**, *30A*, 65–80.